



**Enhanced medium chain length-polyhydroxyalkanoate
production by co-fermentation of lignin and holocellulose
hydrolysates**

| | |
|-------------------------------|--|
| Journal: | <i>Green Chemistry</i> |
| Manuscript ID | GC-ART-07-2021-002725.R1 |
| Article Type: | Paper |
| Date Submitted by the Author: | 13-Sep-2021 |
| Complete List of Authors: | Arreola-Vargas, Jorge; Texas A&M University, Meng, Xianzhi; University of Tennessee, Wang, Yun-Yan; University of Tennessee Knoxville College of Engineering Ragauskas, Arthur; University of Tennessee Knoxville College of Engineering, Yuan, Joshua; Texas A&M University, Institute for Plant Genomics and Biotech |
| | |

Enhanced medium chain length-polyhydroxyalkanoate production by co-fermentation of lignin and holocellulose hydrolysates

Jorge Arreola-Vargas^{a, b}, **Xianzhi Meng**,^c **Yun-yan Wang**,^c **Arthur J. Ragauskas**,^{d, e} **Joshua S. Yuan**^{a, b*}

^a Synthetic and Systems Biology Innovation Hub, Texas A&M University, College Station, TX 77843, USA

^b Department of Plant Pathology and Microbiology, Texas A&M University, College Station, TX 77843, USA

^c Department of Chemical & Biomolecular Engineering, University of Tennessee, Knoxville, TN, 37996, USA

^d Biosciences Division, Oak Ridge National Laboratory, Oak Ridge, TN, 37831, USA

^e Department of Forestry, Wildlife and Fisheries, Center for Renewable Carbon, The University of Tennessee Institute of Agriculture, Knoxville, TN, 37996, USA

*Corresponding author

E-mail address: *syuan@tamu.edu*

Abstract

Biological lignin conversion to medium chain length-polyhydroxyalkanoates (mcl-PHA) has recently emerged as an attractive alternative to petroleum-based plastics due to renewable nature of lignin and value-added applications of mcl-PHA. Previous reports suggested that addition of limited glucose can improve the mcl-PHA accumulation in *Pseudomonas putida* KT2440 grown in lignin substrates. Herein, we proposed a biorefinery process to systematically release lignin and sugars from lignocellulosic biomass and evaluate the potential of co-utilization of all biomass components for conversion to mcl-PHA. Our results indicate that a sequential treatment composed of acid pretreatment, enzymatic hydrolysis and alkaline treatment produces a suitable lignin stream for mcl-PHA production in engineered *P. putida*. Additionally, the PHA titer could be increased 71% when the lignin stream (AH) was combined with the enzymatic hydrolysate (EH) at a ratio 75:25. Higher ratios EH:AH negatively affected the mcl-PHA accumulation as well as mixtures with sugars from the acid hydrolysate. The optimization of the fermentation conditions, including the inoculum (OD_{600}) and substrate (soluble solid content (SSC)), was carried out by a central composite design. Optimal conditions were achieved at $OD_{600}= 2.17$ and $SSC=68.28$ g/L. Under these conditions, the titer increased 4.3 fold, achieving a mcl-PHA production of 1.38 g/L. Lignin characterization before and after fermentation by nuclear magnetic resonance and gas chromatography showed that *p*-coumarates were mainly consumed during the fermentation for mcl-PHA production. Overall, this biorefinery strategy allowed to increase the mcl-PHA production by utilizing the different lignocellulosic fractions. Unlike previous studies no model substrates were utilized at any stage of the fermentation process, representing a step forward towards process feasibility.

Keywords: bioplastics, biorefinery, lignocellulosic biomass, PHA, *Pseudomonas putida*

1 Introduction

Lignocellulosic biomass is an abundant and renewable resource generated throughout the biosphere. Worldwide, 181.5 billion tons of biomass are produced annually, from which approximately 4.6 billion tons correspond to agricultural residues.¹ Rice straw, wheat straw and corn stover are examples of agricultural residues that are left *in-situ* after the harvesting season and are barely valorized. In recent years, these residues have attracted the attention of researchers as alternatives to petroleum-based fuels and bioproducts.²⁻⁴

Current biorefinery approaches from lignocellulosic biomass include pretreatment, saccharification and conversion of the holocellulose (cellulose + hemicellulose) fraction into fuels and chemicals. Lignin is not commonly integrated into this valorization chain because of its polymeric structure constituted of low biodegradable phenyl-propanoid units. However, lignin comprises up to 30% of lignocellulosic biomass, being the most abundant polymer after cellulose.⁵ Therefore, recent research efforts have been focused on lignin valorization⁶⁻¹⁰. According to data obtained in the web of science searching under keywords "*lignin + valorization*", publications in this topic increased more than 2700 % during the last decade going from 17 papers in 2011 to 470 papers in 2020 (Fig. 1). Despite this enormous progress, integral biorefinery schemes are still limited due to the lack of microorganisms capable of efficiently use the different fractions of lignocellulosic biomass and generate value-added products.

Biological lignin conversion to fuels and chemicals was recently proposed as an attractive route for lignin valorization with potential to contribute to the economic feasibility of biorefineries.¹¹⁻¹⁴ By leveraging the metabolic capabilities of bacteria, previous works have shown that carbon from lignin can be funneled to useful products such as medium chain length-polyhydroxyalkanoates (mcl-PHA).^{11,12} Unlike short chain length-polyhydroxyalkanoates (scl-PHA) that have been

widely studied for several years and even commercially developed, the technology for mcl-PHAs production is still under development.^{15,16} mcl-PHA are naturally synthesized polyesters with a chain length ranging from 6 to 14 carbons and have excellent properties to replace petroleum-based plastics. mcl-PHA are biocompatible, biodegradable, and have attractive physical and mechanical properties, since they are elastomers with low crystallinity and low glass transition temperature.¹⁷ Envisioned applications for mcl-PHAs include high value added manufactured goods in biomedical applications, drug delivery, tissue engineering, etc.¹⁸

Pseudomonas putida is one of the main chassis for biological lignin conversion to mcl-PHA because this microorganism is metabolically versatile, degrade lignin via the β -ketoacid pathway and store carbon as mcl-PHA under nutrient limitation.^{19,20} Although lignin bioconversion to mcl-PHA is a relatively new approach for lignin valorization, recent progress has been achieved in this field. Fig. 1 shows that during the last three years, 10 papers have been published in average per year on this topic. Nonetheless, it is worth mentioning that only few works have actually been performed on the conversion of waste lignin to mcl-PHA, since many of the works shown in Fig. 1 were focused on the use of lignin derivatives as model compounds or literature reviews showing the potential, challenges and future directions of this technology.

To the best of our knowledge, biological conversion of waste lignin to mcl-PHA was reported by Linger et al (2014) for the very first time.¹¹ In this work, the authors pretreated corn stover with an alkaline solution to release lignin —whose presence was confirmed by nuclear magnetic resonance (NMR) and gel permeation chromatography (GPC)— and fermented the alkaline pretreated liquor using *P. putida* KT2440. The authors compared the performance of the alkaline pretreated liquor with model substrates obtaining mcl-PHA cell contents from 20 to 39% and mcl-PHA productions from 0.1 to 0.25 g/L. Later on, Lin et al. (2016)²⁰ demonstrated the capacity of

other *P. putida* strains such as *P. putida* A514 to metabolize model or waste lignin and store carbon as mcl-PHA. More recently, our research group reported the effect of combinatorial pretreatment on lignin processability using engineered *P. putida*, achieving mcl-PHA productions up to 1 g/L from alkaline pretreated liquors.²¹ Furthermore, Liu et al. (2019)²² reported the co-fermentation of glucose and lignin to mcl-PHA using *P. putida* KT2440. The authors reported a record mcl-PHA production of 1.5 g/L by using high initial optical densities (OD) of *P. putida* KT2440 pre-cultured in glucose. Despite all this progress, reported works focused mainly on lignin utilization and few studies evaluated the co-utilization of glucose or residual sugar with lignin. It is not clear if cellulose or hemicellulose hydrolysates instead of glucose can improve lignin conversion. This co-fermentation platform can provide an option to convert hydrolysates to either fuels or high value products like mcl-PHA. The new biorefinery strategy allows the adjustment of biorefinery outputs based on market, maximizing the income.

Based on the aforementioned, we hypothesized that the different polymers of the lignocellulosic biomass (hemicellulose, cellulose and lignin) could be potentially funneled to mcl-PHA, allowing full biomass conversion to bioplastics. Therefore, herein we proposed two biomass deconstruction approaches to sequentially release sugars and lignin from corn stover. Then, the potential of both lignin streams was compared for mcl-PHA production by using engineered and wild type *P. putida* strains. Thereafter, co-fermentation of sugars from hemicellulose/cellulose hydrolysates and lignin streams was performed at different ratios aiming mcl-PHA production enhancement. Finally, process optimization was carried out by using a central composite design (CCD), and the structural changes of lignin before and after co-fermentation at optimal conditions were analyzed by NMR and GPC to further understand the fermentation performance.

2 Material and Methods

2.1. Sugar and lignin extraction from corn stover

Corn stover was used as a model lignocellulosic biomass to evaluate mcl-PHA production from agricultural residues. The biomass was collected in Brazos county, Texas U.S after the harvesting season and milled into an average diameter of 1~2 mm by using a laboratory mill. Two biomass deconstruction approaches were followed to release sugars and lignin from milled corn stover. For approach 1, corn stover was submitted to dilute acid pretreatment followed by enzymatic hydrolysis and alkaline treatment. For approach 2, corn stover was submitted to sonication/steam pretreatment followed by alkaline treatment and enzymatic hydrolysis.

In detail, the pretreatment in the approach 1 was carried out with 1% sulfuric acid at 10% solid loading under 121 °C for 60 min using Amsco® LG 250 Laboratory Steam Sterilizer (Steris, USA). For approach 2, the pretreatment was performed by sonication at 50 wt% solid loading, 25 kHz and 65 °C. Thereafter, biomass slurry was treated with steam in a custom pretreatment test set-up by heating biomass at 135 °C at a rate of 2.5 °C/minute and pressurizing to 25 psi at a rate of 0.5 psi/min. Conditions were held for 30 minutes and then the biomass was cooled down.

Enzymatic hydrolysis and alkaline treatment were performed on pretreated biomasses aiming the release of sugars and lignin, respectively. Process conditions were the same for both deconstruction scenarios. In detail, the enzymatic hydrolysis was conducted by using CTec2 and HTec2 (Novozymes, USA) at a volumetric ratio of 10:1 and 10 FPU/g biomass. The solid loading was established at 20% in a 0.05M citrate buffer solution (pH 4.8) at 50 °C and 200 rpm for 168 h. The alkaline treatment was carried out with 1% NaOH at 20% solid loading under 121 °C for 60 min using Amsco® LG 250 Laboratory Steam Sterilizer (Steris, USA).

Sugar and lignin streams were separated by filtration and characterized as mentioned in the

analytical methods section. Lignin streams obtained from deconstruction approaches 1 and 2 are referred as AH1 and AH2 respectively. The acid hydrolysate from approach 1 is referred as Ach while the enzymatic hydrolysate is referred as EH.

2.2 *P. putida* seed cultures

mcl-PHA accumulation in the presence of lignin streams (AH1 and AH2) was firstly evaluated using two *Pseudomonas putida* KT2440 strains, wild type (WT) and an engineered strain (C1J4). C1J4 strain was genetically modified to overexpress genes *phaC1* and *phaJ4* involved in mcl-PHA accumulation as previously described.²⁰ Due to the better performance of this strain compared to WT (section 3.1), C1J4 strain was used for further co-fermentation and optimization experiments. For seed culture preparation, the strain was stored on Luria-Bertani medium containing 1.5% agar. Then, a single colony of the strain was inoculated in 5 mL of Luria-Bertani broth at 30 °C and 180 rpm. After reaching the stationary phase, cells were transferred into 50 mL of M9 mineral medium containing the carbon source (lignin and/or sugars) and the chemicals reported by Liu et al. (2019).²²

2.3 Fermentation/co-fermentation of lignocellulosic hydrolysates for mcl-PHA production

Fermentation of sugar and lignin streams as well as co-fermentation experiments were carried out at same conditions except for the optimization experiments where different initial optical densities (OD_{600}) and soluble solid contents (SSC) were evaluated. In detail, the experiments were carried out in a working volume of 50 mL using 250 mL flasks. Sugars or/and lignin streams adjusted to pH 7 were used as carbon source at a SSC of 20 g/L and mixed with M9 medium. Then, the seed culture was used as inoculum to reach an initial OD_{600} of 0.3. In order to induce high mcl-PHA

productions, the experiments were performed under the fed-batch strategy reported by Liu et al., 2019.²² Fed-batch cycle 1 (18 h) was carried out with nitrogen supply (1.0 g/l NH₄Cl) to favor cell growth and cycle 2 (8 h) was carried out without nitrogen supply to favor mcl-PHA storage inside the cell. After cycle 1 ended, the cells were harvested by centrifugation at 4,000 rpm for 10 min and inoculated in fresh medium at same conditions of cycle 1. At the end of cycle 2, cell biomass was centrifuged at 10,000 rpm for 10 min to determine cell dry weight and PHA content. The fermentation broth was also collected for lignin and sugar analysis. All of the fermentation experiments were carried out by duplicate.

2.4 mcl-PHA extraction and quantification

Cell pellets were recovered after centrifugation and washed with 20 ml 0.9% NaCl solution. Then, the cells were lyophilized for 24 h in a 4.5 L Benchtop Freeze-Dry System (Labconco Corporation, USA). After lyophilization, dry cell biomass was weighted to calculate cell biomass growth. Then, 5-10 mg of lyophilized cells were transferred to screw-cap glass vials to quantify the PHA content by the method reported elsewhere.²⁰⁻²² Briefly, PHAs were extracted with chloroform and subjected to acidic methanolysis (15% v/v H₂SO₄ in CH₃OH) at 100°C for 140 min. Generated hydroxy-methyl esters were recovered within the organic phase and filtered with a 0.45- μ m polytetrafluorethylene (PTFE) membrane. PHA content and relative abundance was obtained by GC-MS (QP2010SE, Shimadzu Scientific Instruments, Inc.) at conditions previously reported.²⁰

2.5 Process optimization by using central composite design (CCD)

The CCD is one of the most renowned designs for optimization of engineering and biotechnological processes.^{23,24} This practical design approaches the optimal response through

sequential experimentation, using factorial designs and then adding axial points to fit second order models (equation 1).

$$Y = \beta_0 + \sum \beta_i x_i + \sum \beta_{ii} x_i^2 + \sum \sum \beta_{ij} x_i x_j + \varepsilon \quad \text{Equation 1}$$

where β_0 is the constant coefficient, β_i is the linear coefficient, β_{ii} is the quadratic coefficient, β_{ij} is the interaction coefficient, Y is the response variable, x represent the independent variables that influence the response variable, and ε is a random error term that accounts for the experimental error.

In this work, a CCD was implemented to optimize two of the most important variables of the co-fermentation of sugars and lignin (SSC and initial OD_{600}). The central levels were selected from our previous experience using lignin as substrate.²² Table 1 shows natural and coded values suggested by the CCD; the response variable was the production of mcl-PHA. Data analysis, response surface plots and analysis of variance (ANOVA) were performed by using the software Statgraphics centurion XV (Statpoint, Technologies, Inc. USA).

2.6 Analytical methods

Lignocellulosic biomass composition was analyzed by using the protocol of the National Renewable Energy Laboratory (NREL). Sugar concentration before and after fermentation was analyzed by HPLC using an Aminex HPX-87P carbohydrate analysis column at conditions previously reported.²¹ Lignin content before and after fermentation was analyzed following the NREL protocol. Besides, lignin derivatives were extracted before and after fermentation with methyl tert-butyl ether (MTBE) and analyzed by GC/MS as previously reported.²¹

Finally, GPC and NMR were employed to determine the molecular weight of the fractionated lignin before and after fermentation as well as the aromatic regions and lignin subunits. Briefly, the molecular weight distributions of acetylated lignin samples were analyzed by an Agilent GPC SECurity 1200 system using a polystyrene standard sample for calibration at conditions previously described.²¹ Regarding NMR, both 2D ¹H–¹³C HSQC and ³¹P were performed using a Bruker Ascend™ 500 MHz spectrometer at conditions previously described.^{25,26}

3 Results and Discussion

3.1. mcl-PHA production from lignin streams

Lignin depolymerization by alkaline pretreatment has been widely investigated aiming the enhancement of cellulose digestibility.^{27–29} According to Gupta and Lee. (2010)²⁷, sodium hydroxide remove lignin from lignocellulosic biomass by hydrolyzing the ether bonds, leaving the cellulose fraction more accessible for enzymatic digestion while solubilizing the lignin fraction in a commonly discarded liquid stream. It was just in recent years that this liquid stream was recognized as a potential substrate for mcl-PHA production given the ability of *P. putida* to degrade aromatic compounds via the β -keto adipate pathway.^{11,20,22} In the present study, we proposed to use two sequential biomass treatments for releasing lignin and sugars from corn stover aiming full biomass conversion to mcl-PHA. The lignocellulosic composition of corn stover was 31.75 ± 2.2 % glucan, 13.01 ± 0.21 % xylan, 4.79 ± 0.24 % arabinan and 24.86 ± 0.03 % lignin. The chemical composition of the lignin streams obtained during both biomass deconstruction approaches is presented in Table 2. Interestingly, AH1 doubled the total lignin content found in AH2, obtaining 23.5 g/L of insoluble lignin and 3.25 g/L of soluble lignin vs. 11.21 g/L of insoluble lignin and 1.7 g/L of soluble lignin, respectively. This difference might be due to 1) the better

performance of the acid pretreatment compared to sonication/steam pretreatment to remove the hemicellulose fraction and enhance the accessibility to lignin and/or 2) the fact that cellulose was enzymatically hydrolyzed prior to the alkaline treatment during the biomass deconstruction approach 1 while for approach 2 the enzymatic hydrolysis was carried out after the alkaline treatment. In both cases, negligible amounts of sugars were found in the alkaline hydrolysates (Table 2).

The potential of these two lignin streams was firstly evaluated for mcl-PHA accumulation in two *P. putida* strains. Fig. 2 shows that strain C1J4 produces 52% more mcl-PHA compared to wild type strain when AH1 is used as substrate. Both strains produced similar amounts of cell biomass; however, the mcl-PHA intracellular content increased from 13% in wild type to 19% in C1J4. Previous works in our research group have reported a similar trend when WT and C1J4 were cultured in vanillic acid, a phenolic model substrate.²⁰ On the other hand, the intracellular mcl-PHA content also agrees with previous reports using alkaline hydrolysate as substrate. For instance, Salvachúa et al (2019)¹² reported a mcl-PHA content of 17.7% by using a lignin stream and engineered *P. putida*.

Interestingly, cell biomass and mcl-PHA content decreased significantly when AH2 was used as substrate. Fig. 2 shows that biomass production in C1J4 decreased 41% when AH2 was used as substrate compared to AH1, while the mcl-PHA content decreased 56%. In agreement with this trend, the mcl-PHA production and mcl-PHA yield with AH2 resulted much lower compared to AH1. mcl-PHA yields obtained with AH1 agree with values reported in our previous work²² and are 3 to 4 times higher than experiments with AH2. The presence of other components such as oligosaccharides and extractives as well as the lower lignin content in AH2 compared to AH1 (Table 2) could explain the lower mcl-PHA yields, since the experiments were standardized in

terms of SSC. Previous studies have reported mcl-PHA contents up to 70% by using model lignin chemicals¹⁵. In fact, our data suggests that lignin from the alkaline hydrolysate is a highly recalcitrant biopolymer and even when AH1 is used as substrate, the removal reaches only \square 30%, suggesting that further treatment is needed to depolymerize long-chain-length lignin fractions to oligo or monolignols. In this context, our previous studies^{22,30,31} suggested that the addition of laccases from *Trametes versicolor* can help to further depolymerize the lignin stream, improving lignin digestibility. Therefore, in order to increase lignin consumption, mcl-PHA accumulation and avoid mcl-PHA depolymerization, future works are encouraged on the use of lignin streams depolymerized with laccases, or the use of engineered *P. putida* strains with secretory expression of laccase enzymes.³² Additional strategies include engineering strains to avoid PHA degradation via phaZ gene knocked out.³³

3.2. Effect of sugars from the hemicellulose and cellulose fractions as co-substrates for the conversion of lignin into mcl-PHA

Because of the better performance obtained with AH1 for mcl-PHA production, sugar streams from deconstruction approach 1 were evaluated as substrates and co-substrates during fermentation. The chemical composition of the acid and enzymatic hydrolysates are presented in Table 2. The main sugars of the AcH were xylose and arabinose, which agrees with the main depolymerized fraction during dilute acid hydrolysis, i.e. hemicellulose.³⁴ The difference between the sums of mono/di-saccharides and the SSC could be due to presence of oligosaccharides and other components from the extractives like pectin and proteins, as well as ash. On the other hand, during the enzymatic hydrolysis, glucose was the main released sugar followed by xylose. The high sugar content in this hydrolysate highlights the efficiency of the enzymatic process to release sugars from

the cellulose and the remaining hemicellulose fractions.

Fig. 3 shows the performance of these two hydrolysates during fermentation with WT and C1J4. Both strains grown in AcH accumulated insignificant amounts of mcl-PHA even though the growth was only slightly lower compared to strains grown in EH. Probable reasons for the low mcl-PHA production include the presence of extractives, pectin, oligosaccharides and some toxic compounds in AcH³⁵. Even though furfural and hydroxymethyl furfural were not detected in this hydrolysate, acetic acid was found at a concentration of 0.3 g/L. In addition, *P. putida* KT2440 is not able to naturally assimilate pentoses.^{36,37} Interestingly, the highest mcl-PHA content observed in C1J4 using EH resulted much lower compared to the use of the lignin stream (AH1), 8.5% vs. 19% respectively. This result could be linked to the acidification of the medium due to high production of acetic acid during the fermentation of glucose—the pH dropped to 5.6 in the experiment with EH— but also highlights the potential of the lignin stream for mcl-PHA accumulation.

Fig. 4 shows the co-fermentation of both hydrolysates with the lignin stream AH1 by using the C1J4 strain. The co-fermentation experiments with lignin stream and acid hydrolysate presented in Fig. 4A confirms the negative effect caused by the presence of the AcH components. In agreement with the experiment using sole AcH, cell biomass increased at higher ratios AcH:AH but mcl-PHA content decreased to values below 5% even in the presence of only 25% AcH. Interestingly, the relative abundance of mcl-PHA changes from a dominance of 3-hydroxydodecanoic acid (C12) in the presence of sole AH to 3-hydroxyhexanoic acid (C6) when AH is being replaced by AcH. This change on the mcl-PHA relative abundance agrees with the mcl-PHA composition presented in Fig. 2 and 3 for AH and AcH, respectively. Previous works have demonstrated that mcl-PHA monomers (hydroxyalkanoates) with a larger carbon chain are

predominant when lignin streams are fermented¹². However, the dynamic on the production of these hydroxyalkanoates when lignin stream is partially substituted by hemicellulose byproducts is reported for the very first time and suggests changes in the metabolic pathway, which agrees with the variability on PHA composition reported when different carbon sources are used as substrate.³⁸

Regarding the co-fermentation experiments with the enzymatic hydrolysate, Fig. 4B shows that the highest mcl-PHA production was achieved at a 75/25 AH:EH ratio, at this condition 0.55 g/L of mcl-PHA were produced and no significant difference was found between the mcl-PHA content of this mixture and the experiment with sole AH ($P=0.214$). Even though the cell biomass increased at higher AH:EH ratios, the mcl PHA content decreased due to acidification similarly to experiment with sole EH. In agreement with the experiments using sole AH or EH (Fig. 3), the main mcl-PHA monomer during the co-fermentation experiments was 3-hydroxydodecanoic acid. Finally, it is worth mentioning that yields presented in Fig. 4 during the co-fermentation experiments are clearly overestimated due to the presence of sugars that are also used as substrate for PHA production.³⁹

3.3. Optimization of the co-fermentation process by CCD

Since the best mcl-PHA production was achieved at a ratio 75 AH:25 EH—representing a 71% improvement compared to the use of sole AH—, we used this mixture for optimizing the fermentation conditions. A CCD was employed to optimize the process and determine the individual and interaction effects of the inoculum and substrate content, measured as OD_{600} and SSC, respectively. It is important to mention that in order to increase the OD_{600} , the C1J4 strain after initial cultivation in LB medium was pre-cultured in EH aiming high cell biomass production

and full utilization of lignocellulose streams. This differs from previous studies in which this pre-culture step was carried out using glucose.²² Table 2 shows the responses obtained for cell biomass growth and mcl-PHA content as well as the total mcl-PHA production. Interestingly, the highest mcl-PHA content was reached at the lowest tested OD₆₀₀, while in general high SSC favored cell biomass growth. Overall, both variables showed to strongly influence the mcl-PHA production, obtaining titers from 0.49 to 1.33 g/L.

The Equation 2 shows the simplest second order model that accurately represent the experimental data, given the adjusted R² value of 0.9 and p-value of 0.0034, indicating an adequate fitting with 95% of confidence. Fig. 5A shows the observed data (experimental) vs. the predicted data by the model where a close approximation can be observed. On the other hand, Fig. 5B shows the response surface generated by using the second order model. This Figure shows a clear trend to increase the mcl-PHA production at low OD₆₀₀ and high SSC, while the lowest mcl-PHA production is observed at lowest values of both independent variables. The ANOVA shows that both variables OD₆₀₀ and SSC were significant at a 95% confidence interval, given their p-values 0.0373 and 0.0471 (Table S1). Furthermore, also the interaction between both variables resulted significant (p= 0.0055), which highlights the relevance of using elaborated experimental designs like the CCD instead of multiple one-factor designs where the interaction cannot be assessed. Moreover, one-factor at a time designs are commonly time and resource-consuming options when multiple variables are optimized.⁴⁰

$$mclPHA = -0.142235 + 0.0544867 * SSC + 0.0186702 * OD * OD - 0.000246337 * SSC * SSC - 0.00598568 * SSC * OD$$

Equation 2

The stationary point in the response surface or in other words the optimal mcl-PHA production was predicted at 1.62 g /L. Fig. 5b shows this value can be theoretically achieved at an OD₆₀₀ of 2.17 and a SSC of 68.28 g/L. Interestingly, the suggested optimal SSC is close to the highest concentration that can be reached in the fermentation medium by taking into account the undiluted concentrations of the mixture. This evidences the capacity of the C1J4 strain to grow under high concentrations of lignin derivatives while accumulates mcl-PHA as inclusion bodies due to the nitrogen limitation,⁴¹ since nitrogen supply was maintained constant during all the performed experiments.

3.4. Experimental analysis at predicted optimal conditions and structural changes of lignin during fermentation

Predicted optimal conditions were evaluated experimentally using two approaches for the pre-culture of the C1J4 strain. Both approaches were evaluated at same fermentation conditions (75 AH:25 EH, OD₆₀₀=2.17 and SSC=68.28 g/L) except that in one the C1J4 strain was pre-cultured in EH while in the other it was pre-cultured in AcH. The main reason to evaluate the pre-culture in AcH is the fact that AcH promoted the growth of *P. putida* even though mcl-PHA was not accumulated (Fig. 3). Fig. 6 shows that after fermentation the mcl-PHA content of cells pre-cultured in AcH resulted much lower compared to the mcl-PHA content of cells pre-cultured in EH, 9% vs. 23%, respectively. This result is interesting because apparently the pre-culture step greatly influenced the capacity of the cells to accumulate mcl-PHA even when the main fermentation step is carried out with a suitable substrate (mixture AH:EH) at optimal conditions. Future detoxification studies could be implemented to determine the main cause of the negative effect of the AcH and increase the mcl-PHA accumulation during fermentation. In this regard,

different detoxification methods are widely available in the literature for acid hydrolysates, including: evaporation, overliming, ion exchange resins and adsorption.⁴²

Cells pre-cultured in EH and cultured at optimal conditions predicted by the CCD experiments accumulated 23% mcl-PHA and produced a mcl-PHA titer of 1.38 g/L, resulting slightly lower than the predicted optimum. Nonetheless, it represents a 4.3 fold increase compared to the initial experiment with sole AH, both with a dominance of 3-hydroxydodecanoic acid monomer. Interestingly, our optimal mcl-PHA production is similar to the highest mcl-PHA production (1.5 g/L) reported by Liu et al (2019)²² by using AH as substrate and glucose as pre-culture step, which highlights the result of the present study where different components of the lignocellulosic biomass were used as substrate and no exogenous carbon source was used for pre-culture.

The main component of the EH, i.e. glucose, was completely consumed at the end of this experiment at optimal conditions. However, the consumption of lignin by *P. putida* implies the generation of lignin degrading enzymes as well as the use of peripheral pathways to transform the lignin derivatives to intermediates of the central metabolism via the β -keto adipate pathway.^{11,20} According to Fig. S1, the main lignin derivatives found in AH were coumaran, ethanone and coumaric acid, which were 70%, 60% and 90% removed after fermentation, respectively. These lignin derivatives have been previously reported as the main components of alkaline lignin streams and can be subjected to degradation and bioconversion in different bacterial species including *Rhodococcus opacus* and other *P. putida* strains.^{31,43}

Lignin bioconversion is influenced by many factors including the molecular weight of this biopolymer. Table 4 shows that both the weight-average (M_w) and number-average (M_n) molecular weight as well as the polydispersity index (PDI) decreased in AH compared to native lignin in corn stover (CSNL) due to fractionation, which is in agreement with previous reports.^{44–46}

Interestingly, M_w increased in the sample after fermentation and M_n remained relatively constant, which can be apparently due to the consumption of lower molecular weight lignin by *P. putida*, agreeing with previous findings during laccase treatment or fermentation with *Rhodococci* and *P. putida*.^{22,30,31,47}

Fig. 7 and Table 5 shows that compared to CSNL, AH increases the H-lignin content, which favors the consumption by lignin-degrading bacteria⁴⁸ and agrees with our previous observations.²² Then, as expected H-lignin decreased after fermentation from 18.3 to 15.8 % while S and G-lignin subunits remained unchanged. Interestingly, both ferulates and *p*-coumarates increased in the fractionated lignin (AH) compared to CSNL but only the *p*-coumarates were significantly consumed (94%) during the fermentation with *P. putida* for mcl-PHA production. The latter agrees 1) with the results obtained by GC-MS, 2) with a previous study that demonstrated the preference of *P. putida* for consumption of coumaric acid over ferulic acid¹¹ and 3) with previous observations in our research group using lignin streams.²² It is interesting that *P. putida* prefers coumaric acid over ferulic acid despite that both compounds follow the same β -ketoacid pathway from the same intermediary protocatechuic acid, suggesting that this preference is triggered by upper metabolic pathways. Regarding lignin linkages, the alkaline treatment reduced the content of β -O-4 and β - β linkages, which agrees with the decrease of the molecular weight of fractionated lignin compared to CSNL. However, only the β - β linkage was further reduced after fermentation. Finally, the contents of various hydroxyl groups in lignin before and after fermentation were obtained by a quantitative ³¹P NMR analysis (Fig. 8). Results showed an increase on the content of phenolic and aliphatic OH groups after fermentation, while COOH groups slightly decreased. Among the phenolic OH groups, C₅-substituted OH including the syringyl and other types of condensed 5-substituted units (e.g., 5-5 and β -5) was observed as the most predominant OH group.

The increase in phenolic OH group after fermentation could be due to cleavage of aryl-ether linkage and further depolymerization of lignin. Previous studies have reported similar behaviors, obtaining increases in OH groups after lignin fermentation in *R. opaccus*.⁴⁹

In summary, the bioconversion of lignin streams and sugar-rich hydrolysates to mcl-PHA provides an attractive alternative to current biorefinery schemes. Even though our PHA titer is slightly lower compared to that obtained by Liu et al (2019)²² (1.38 g/L vs. 1.5 g/L), we did not use model substrates like glucose at any stage of the fermentation process, representing an enormous advantage for future commercialization of the technology. Moreover, the co-utilization of both fractions of the biomass (lignin and holocellulose) for mcl-PHA production could serve as an attractive option for biorefinery companies to cope with the volatile market and price of biofuels.

4. Conclusions

A novel biorefinery platform for bioconversion of lignin and holocellulose fractions to mcl-PHA aiming full biomass conversion to bioplastics is presented in this work. Our results indicated that mcl-PHA accumulation was favored in the presence of lignin streams while sugar-rich hydrolysates mainly promoted cell biomass growth. Nonetheless, combined at an appropriate ratio, both lignocellulosic streams can synergize to increase the mcl-PHA production. Compared to sole lignin stream, the titer increased 71% when this lignin stream was combined with the enzymatic hydrolysate at a ratio 75:25. Furthermore, the titer increased 4.3 fold when optimal fermentation conditions were used, achieving a mcl-PHA production of 1.38 g/L. The NMR analysis suggested that *p*-coumarates were mainly consumed through β -keto adipate pathway to form mcl-PHA. Overall, sugar and lignin streams demonstrated their potential to boost mcl-PHA production providing another alternative to current biorefinery platforms.

CRedit authorship contribution statement

JAV: Conceptualization, investigation, methodology, data curation, formal analysis, validation, writing-original draft; XM, YYW and AJR: Data curation, formal analysis, writing-review and editing; JSY: Conceptualization, funding acquisition, project administration, resources, supervision, writing-review and editing.

Conflict of interest

The authors declare no competing financial interests

Acknowledgements

Arreola-Vargas J. thanks CONACYT for the postdoctoral fellowship. This work was financially supported by the U.S. DOE (Department of Energy) EERE (Energy Efficiency and Renewable Energy) BETO (Bioenergy Technology Office) (Grant No. DE-EE0006112, DE-EE0007104, and DE-EE0008250). Oak Ridge National Laboratory is managed by UT-Battelle, LLC under Contract DE-AC05-00OR22725 with the U.S. Department of Energy (DOE). The views and opinions of the authors expressed herein do not necessarily state or reflect those of the United States Government or any agency thereof. Neither the United States Government nor any agency thereof, nor any of their employees, makes any warranty, expressed or implied, or assumes any legal liability or responsibility for the accuracy, completeness, or usefulness of any information, apparatus, product, or process disclosed, or represents that its use would not infringe privately owned rights. The United States Government retains and the publisher, by accepting the article for publication, acknowledges that the United States Government retains a non-exclusive, paid-up,

irrevocable, worldwide license to publish or reproduce the published form of this manuscript, or allow others to do so, for United States Government purposes. The Department of Energy will provide public access to these results of federally sponsored research in accordance with the DOE Public Access Plan (<http://energy.gov/downloads/doe-public-access-plan>).

References

- 1 N. Dahmen, I. Lewandowski, S. Zibek and A. Weidtmann, *GCB Bioenergy*, 2019, **11**, 107–117.
- 2 E. Virmond, R. F. De Sena, W. Albrecht, C. A. Althoff, R. F. P. M. Moreira and H. J. José, *Waste Manag.*, 2012, **32**, 1952–1961.
- 3 Z. Zhang, J. Song and B. Han, *Chem. Rev.*, 2017, **117**, 6834–6880.
- 4 U. De Corato, I. De Bari, E. Viola and M. Pugliese, *Renew. Sustain. Energy Rev.*, 2018, **88**, 326–346.
- 5 S. Lee, M. Kang, J. H. Bae, J. H. Sohn and B. H. Sung, *Front. Bioeng. Biotechnol.*, 2019, **7**, 209.
- 6 Z. H. Liu, R. K. Le, M. Kosa, B. Yang, J. Yuan and A. J. Ragauskas, *Renew. Sustain. Energy Rev.*, 2019, **105**, 349–362.
- 7 Z.-H. Liu, N. Hao, S. Shinde, Y. Pu, X. Kang, A. J. Ragauskas and J. S. Yuan, *Green Chem.*, 2019, **21**, 245–260.
- 8 S. Xie, Q. Li, P. Karki, F. Zhou and J. S. Yuan, *ACS Sustain. Chem. Eng.*, 2017, **5**, 2817–2823.
- 9 Q. Li, C. Hu, M. Li, P. Truong, M. T. Naik, D. Prabhu, L. Hoffmann, W. L. Rooney and J. S. Yuan, *iScience*, 2020, **23**, 101405.
- 10 Z.-H. Liu, N. Hao, Y.-Y. Wang, C. Dou, F. Lin, R. Shen, R. Bura, D. B. Hodge, B. E. Dale, A. J. Ragauskas, B. Yang and J. S. Yuan, *Nat. Commun.* 2021 121, 2021, **12**, 1–13.
- 11 J. G. Linger, D. R. Vardon, M. T. Guarnieri, E. M. Karp, G. B. Hunsinger, M. A. Franden, C. W. Johnson, G. Chupka, T. J. Strathmann, P. T. Pienkos and G. T. Beckham, *Proc. Natl. Acad. Sci. U. S. A.*, 2014, **111**, 12013–12018.

- 12 D. Salvachúa, T. Rydzak, R. Auwae, A. De Capite, B. A. Black, J. T. Bouvier, N. S. Cleveland, J. R. Elmore, A. Furches, J. D. Huenemann, R. Katahira, W. E. Michener, D. J. Peterson, H. Rohrer, D. R. Vardon, G. T. Beckham and A. M. Guss, *Microb. Biotechnol.*, 2020, **13**, 290–298.
- 13 A. J. Ragauskas, G. T. Beckham, M. J. Bidy, R. Chandra, F. Chen, M. F. Davis, B. H. Davison, R. A. Dixon, P. Gilna, M. Keller, P. Langan, A. K. Naskar, J. N. Saddler, T. J. Tschaplinski, G. A. Tuskan and C. E. Wyman, *Science (80-.)*, 2014, 344.
- 14 G. T. Beckham, C. W. Johnson, E. M. Karp, D. Salvachúa and D. R. Vardon, *Curr. Opin. Biotechnol.*, 2016, 42, 40–53.
- 15 Q. Wang and C. T. Nomura, *J. Biosci. Bioeng.*, 2010, **110**, 653–659.
- 16 M. Singh, P. Kumar, S. Ray and V. C. Kalia, *Indian J. Microbiol.*, 2015, 55, 235–249.
- 17 V. Montiel-Corona and G. Buitrón, *Bioresour. Technol.*, 2021, 323, 124610.
- 18 Z. A. Raza, S. Abid and I. M. Banat, *Int. Biodeterior. Biodegrad.*, 2018, 126, 45–56.
- 19 Z. Xu, X. Li, N. Hao, C. Pan, L. de la torre, A. Ahamed, J. H. Miller, A. J. Ragauskas, J. Yuan and B. Yang, *Bioresour. Technol.*, 2019, **273**, 538–544.
- 20 L. Lin, Y. Cheng, Y. Pu, S. Sun, X. Li, M. Jin, E. A. Pierson, D. C. Gross, B. E. Dale, S. Y. Dai, A. J. Ragauskas and J. S. Yuan, *Green Chem.*, 2016, **18**, 5536–5547.
- 21 Z. H. Liu, M. L. Olson, S. Shinde, X. Wang, N. Hao, C. G. Yoo, S. Bhagia, J. R. Dunlap, Y. Pu, K. C. Kao, A. J. Ragauskas, M. Jin and J. S. Yuan, in *Innovations of Green Process Engineering for Sustainable Energy and Environment 2017 - Topical Conference at the 2017 AIChE Annual Meeting*, AIChE, 2017, vol. 2017-October, pp. 248–264.
- 22 Z. H. Liu, S. Shinde, S. Xie, N. Hao, F. Lin, M. Li, C. G. Yoo, A. J. Ragauskas and J. S. Yuan, *Sustain. Energy Fuels*, 2019, **3**, 2024–2037.
- 23 L. Breton-Deval, H. O. Méndez-Acosta, V. González-Álvarez, R. Snell-Castro, D. Gutiérrez-Sánchez and J. Arreola-Vargas, *J. Environ. Manage.*, 2018, **224**, 156–163.
- 24 M. Mäkelä, *Energy Convers. Manag.*, 2017, **151**, 630–640.
- 25 C. Gong, N. Bryant, X. Meng, S. Bhagia, Y. Pu, D. Xin, C. B. Koch, C. Felby, L. G. Thygesen, A.

- Ragauskas and S. T. Thomsen, *Green Chem.*, 2021, **23**, 1050–1061.
- 26 X. Meng, C. Crestini, H. Ben, N. Hao, Y. Pu, A. J. Ragauskas and D. S. Argyropoulos, *Nat. Protoc.* 2019 149, 2019, **14**, 2627–2647.
- 27 R. Gupta and Y. Y. Lee, *Bioresour. Technol.*, 2010, **101**, 8185–8191.
- 28 J. Singh, M. Suhag and A. Dhaka, *Carbohydr. Polym.*, 2015, 117, 624–631.
- 29 J. Arreola-Vargas, E. Razo-Flores, L. B. Celis and F. Alatrliste-Mondragón, *Int. J. Hydrogen Energy*, 2014, **40**, 10756–10765.
- 30 S. Xie, Q. Sun, Y. Pu, F. Lin, S. Sun, X. Wang, A. J. Ragauskas and J. S. Yuan, *ACS Sustain. Chem. Eng.*, 2017, **5**, 2215–2223.
- 31 Z. H. Liu, S. Xie, F. Lin, M. Jin and J. S. Yuan, *Biotechnol. Biofuels*, 2018, **11**, 21.
- 32 S. Xie, S. Sun, F. Lin, M. Li, Y. Pu, Y. Cheng, B. Xu, Z. Liu, L. da C. Sousa, B. E. Dale, A. J. Ragauskas, S. Y. Dai and J. S. Yuan, *Adv. Sci.*, 2019, **6**, 1801980.
- 33 L. I. De Eugenio, P. García, J. M. Luengo, J. M. Sanz, J. S. Román, J. L. García and M. A. Prieto, *J. Biol. Chem.*, 2007, **282**, 4951–4962.
- 34 D. Kumari and R. Singh, *Renew. Sustain. Energy Rev.*, 2018, **90**, 877–891.
- 35 F. Horlamus, Y. Wang, D. Steinbach, M. Vahidinasab, A. Wittgens, F. Rosenau, M. Henkel and R. Hausmann, *GCB Bioenergy*, 2019, **11**, 1421–1434.
- 36 Y. Wang, F. Horlamus, M. Henkel, F. Kovacic, S. Schläfle, R. Hausmann, A. Wittgens and F. Rosenau, *GCB Bioenergy*, 2019, **11**, 249–259.
- 37 P. Dvořák, J. Kováč and V. de Lorenzo, *Microb. Biotechnol.*, 2020, **13**, 1273–1283.
- 38 G. Jiang, D. J. Hill, M. Kowalczyk, B. Johnston, G. Adamus, V. Irorere and I. Radecka, *Int. J. Mol. Sci.*, 2016, 17.
- 39 S. Munir and N. Jamil, *J. Basic Microbiol.*, 2018, **58**, 247–254.
- 40 Z. Li, D. Lu and X. Gao, *J. Build. Eng.*, 2021, 36, 102101.
- 41 D. Jendrossek and D. Pfeiffer, *Environ. Microbiol.*, 2014, 16, 2357–2373.
- 42 E. Palmqvist and B. Hahn-Hägerdal, *Bioresour. Technol.*, 2000, **74**, 17–24.

- 43 S. Tomizawa, J. A. Chuah, K. Matsumoto, Y. Doi and K. Numata, *ACS Sustain. Chem. Eng.*, 2014, **2**, 1106–1113.
- 44 G. Hu, C. Cateto, Y. Pu, R. Samuel and A. J. Ragauskas, in *Energy and Fuels*, American Chemical Society, 2012, vol. 26, pp. 740–745.
- 45 B. B. Hallac, Y. Pu and A. J. Ragauskas, in *Energy and Fuels*, American Chemical Society, 2010, vol. 24, pp. 2723–2732.
- 46 X. Meng, A. Parikh, B. Seemala, R. Kumar, Y. Pu, P. Christopher, C. E. Wyman, C. M. Cai and A. J. Ragauskas, *ACS Sustain. Chem. Eng.*, 2018, **6**, 8711–8718.
- 47 M. Kosa and A. J. Ragauskas, *Green Chem.*, 2013, **15**, 2070–2074.
- 48 T. Wells and A. J. Ragauskas, *Trends Biotechnol.*, 2012, 30, 627–637.
- 49 Z. Wei, G. Zeng, F. Huang, M. Kosa, D. Huang and A. J. Ragauskas, *Green Chem.*, 2015, **17**, 2784–2789.

Tables

Table 1. Natural and coded values used in the central composite design for mcl-PHA optimization

| Variable | Coded symbol | Coded level | | | | |
|-------------------|--------------|-------------|----|----|----|------------|
| | | $-\alpha^a$ | -1 | 0 | 1 | α^a |
| OD ₆₀₀ | X1 | 2.2 | 3 | 5 | 7 | 7.8 |
| SSC (g/L) | X2 | 11.7 | 20 | 40 | 60 | 68 |

^a α (axial distance) = $4\sqrt{n_f} = 1.414$, where n_f is the number of experiments of the factorial design

Table 2. Chemical composition of the acid, enzymatic and alkaline hydrolysates used for mcl-
PHA production

| Components (g/L) | AcH | EH | AH1 | AH2 |
|--------------------------|----------|-----------|-----------|-----------|
| Acid insoluble lignin | * | * | 23.50±1.4 | 11.21±1.1 |
| Acid soluble lignin | * | * | 3.25±0.1 | 1.70±0.0 |
| Cellobiose | 1.39±0.1 | 0.62±0.0 | 0.15±0.0 | 0.19±0.0 |
| Glucose | 0.56±0.0 | 54.21±1.4 | 0.13±0.0 | 0.15±0.0 |
| xylose | 4.77±0.1 | 10.2±0.2 | ND | ND |
| Galactose | 0.18±0.0 | ND | ND | ND |
| Arabinose | 2.99±0.1 | ND | ND | ND |
| SSC | 34.5±0.8 | 78.8±1.2 | 99.9±8.9 | 49.8±0.6 |

ND=Not detected; *=Not determined; SSC=Soluble solid content; AcH= Acid hydrolysate; EH= Enzymatic hydrolysate; AH1=Alkaline hydrolysate 1; AH2=Alkaline hydrolysate 2.

Table 3. Responses obtained during the fermentation of the alkaline/enzymatic hydrolysate mixture (75:25) at different conditions of initial OD₆₀₀ and SSC suggested by the CCD

| Run | Coded symbol and level | | PHA content (g/g) | Cell biomass growth (g/L) | PHA production (g/L) |
|-----|------------------------|----|-------------------|---------------------------|----------------------|
| | X1 | X2 | | | |
| 1 | 0 | 0 | 0.165 ± 0.015 | 6.20 ± 0.1 | 1.02 ± 0.07 |
| 2 | 0 | 0 | 0.163 ± 0.013 | 5.60 ± 0.35 | 0.91 ± 0.13 |
| 3 | 0 | 0 | 0.138 ± 0.016 | 6.02 ± 0.08 | 0.83 ± 0.06 |
| 4 | -1 | -1 | 0.150 ± 0.005 | 4.98 ± 0.22 | 0.75 ± 0.01 |
| 5 | 1 | -1 | 0.139 ± 0.019 | 6.88 ± 0.13 | 0.96 ± 0.05 |
| 6 | -1 | 1 | 0.191 ± 0.01 | 6.96 ± 0.24 | 1.33 ± 0.11 |
| 7 | 1 | 1 | 0.073 ± 0.003 | 7.64 ± 0.14 | 0.56 ± 0.01 |
| 8 | -α | 0 | 0.197 ± 0.024 | 5.76 ± 0.25 | 1.134 ± 0.1 |
| 9 | α | 0 | 0.116 ± 0.004 | 8.16 ± 0.16 | 0.95 ± 0.01 |
| 10 | 0 | -α | 0.110 ± 0.01 | 4.48 ± 0.12 | 0.49 ± 0.04 |
| 11 | 0 | α | 0.130 ± 0.018 | 7.04 ± 0.46 | 0.92 ± 0.17 |

Table 4. Molecular weight distributions of the CSNL and the fractionated lignin before and after fermentation under optimal conditions

| Sample | Before fermentation | | | After fermentation | | |
|--------|---------------------|---------------|-----|--------------------|---------------|-----|
| | M_w (g/mol) | M_n (g/mol) | PDI | M_w (g/mol) | M_n (g/mol) | PDI |
| CSNL | 12230 | 2521 | 4.9 | | | |
| AH1 | 3347 | 1270 | 2.6 | 8334 | 1246 | 6.7 |

CSNL=corn stover native lignin; M_w =weight-average molecular weight; M_n =Number-average molecular weight; PDI= Polydispersity index

Table 5. Semiquantitative analysis of lignin subunits, end groups and inter-unit linkages in lignin samples before and after fermentation at optimal conditions

| Parameter | Before fermentation | After fermentation | CSNL |
|-------------------------|---------------------|--------------------|-------|
| Lignin subunits (%) | | | |
| Syringyl (S) | 47.40 | 48.40 | 47.60 |
| Guaiacyl (G) | 34.30 | 34.35 | 50.50 |
| p-hydroxyl (H) | 18.30 | 15.80 | 1.90 |
| S/G ratio | 1.38 | 1.41 | 0.94 |
| End groups (%) | | | |
| Ferulates (FA) | 10.50 | 9.85 | 2.10 |
| p-coumarates (PCA) | 28.90 | 1.80 | 16.80 |
| Inter-unit linkages (%) | | | |
| β -O-4 | 31.90 | 34.35 | 42.20 |
| β - β | 1.25 | 0.85 | 2.70 |
| β -5 | 2.70 | 2.85 | 2.00 |

CSNL=corn stover native lignin; Content (%) expressed as a fraction of S+G+H.

Figure captions

Fig. 1. Papers published during the last 10 years on the valorization of lignin and conversion to PHA. Source: ISI Web of knowledge.

Fig. 2. Fermentation performance of WT and C1J4 strains during the conversion of alkaline hydrolysates (AH1 and AH2) to mcl-PHA. Experiments were performed at 20 g/L SSC, pH 7 and initial OD₆₀₀=0.3. A) PHA and Cell biomass production; B) lignin removal and PHA yield; C) PHA relative abundance and PHA content.

Fig. 3. Fermentation performance of WT and C1J4 strains during the conversion of acid (AcH) and enzymatic (EH) hydrolysates to mcl-PHA. Experiments were performed at 20 g/L SSC, pH 7 and initial OD₆₀₀=0.3. A) PHA and Cell biomass production; B) PHA relative abundance and PHA content.

Fig. 4. Effect of A) acid (AcH) and B) enzymatic (EH) hydrolysates as co-substrates during the conversion of lignin (AH) to mcl-PHA in C1J4. Experiments were performed at 20 g/L SSC, pH 7 and initial OD₆₀₀=0.3; ratios are expressed in terms of SSC. A1 and B1) PHA and Cell biomass production; A2 and B2) lignin removal and PHA yield; A3 and B3) PHA relative abundance and PHA content.

Fig. 5. A) Fitting of the quadratic model (Eqn. 2) to experimental data during the central composite design, and B) response surface obtained from the quadratic model (Eqn. 2) with optimal conditions displayed.

Fig. 6. Experimental evaluation of optimal conditions predicted by the quadratic model (Eqn. 2) by using acid (AcH) and enzymatic (EH) hydrolysates to pre-culture C1J4 strain. A) PHA and Cell

biomass production; B) PHA relative abundance and PHA content.

Fig. 7. The 2D HSQC NMR spectra of CSNL, and AH before and after fermentation.

Fig. 8. Quantification of different hydroxyl group contents (mmol/g) in lignin samples before and after fermentation under optimal conditions determined by ^{31}P NMR spectra.

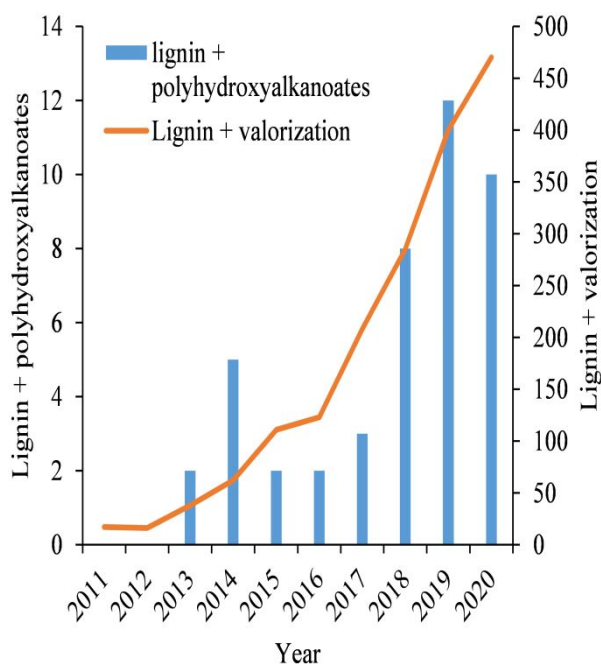


Fig. 1. Papers published during the last 10 years on the valorization of lignin and conversion to PHA. Source: ISI Web of knowledge.

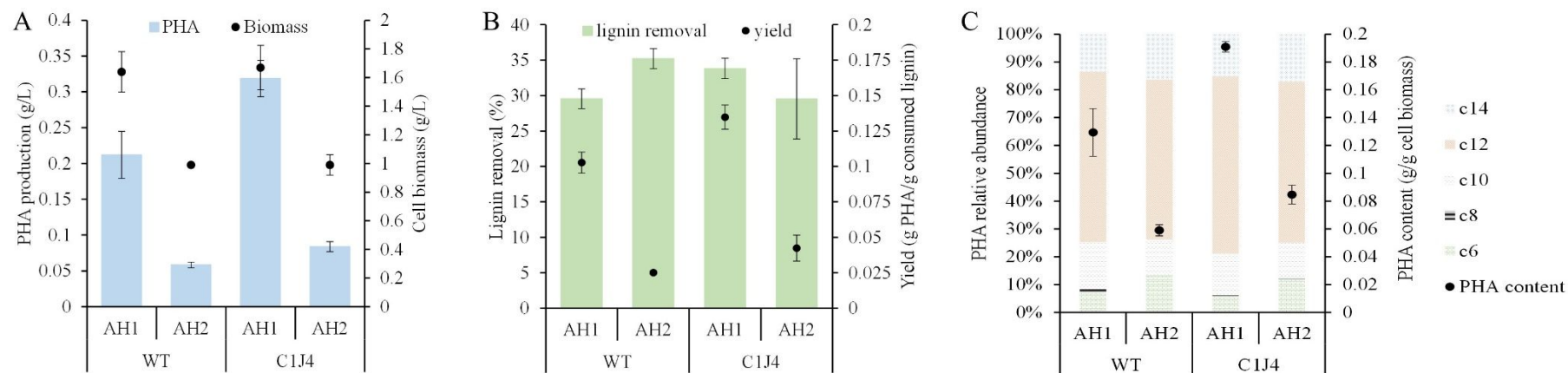


Fig. 2. Fermentation performance of WT and C1J4 strains during the conversion of alkaline hydrolysates (AH1 and AH2) to mcl-PHA. Experiments were performed at 20 g/L SSC, pH 7 and initial $OD_{600}=0.3$. A) PHA and Cell biomass production; B) lignin removal and PHA yield; C) PHA relative abundance and PHA content.

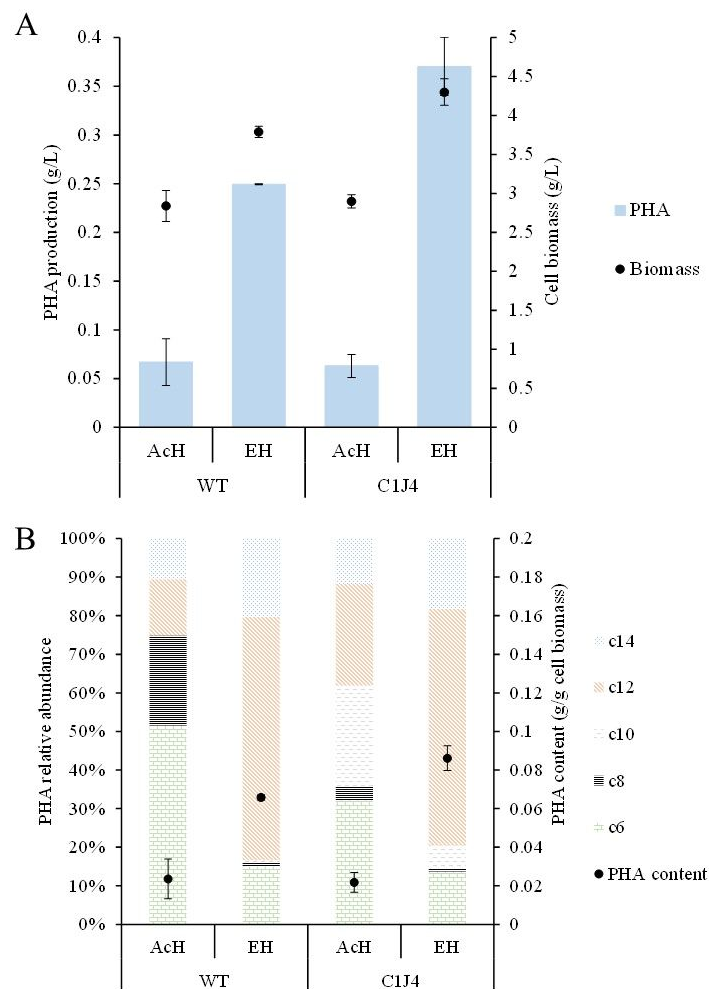


Fig. 3. Fermentation performance of WT and C1J4 strains during the conversion of acid (AcH) and enzymatic (EH) hydrolysates to mcl-PHA. Experiments were performed at 20 g/L SSC, pH 7 and initial $OD_{600}=0.3$. A) PHA and Cell biomass production; B) PHA relative abundance and PHA content.

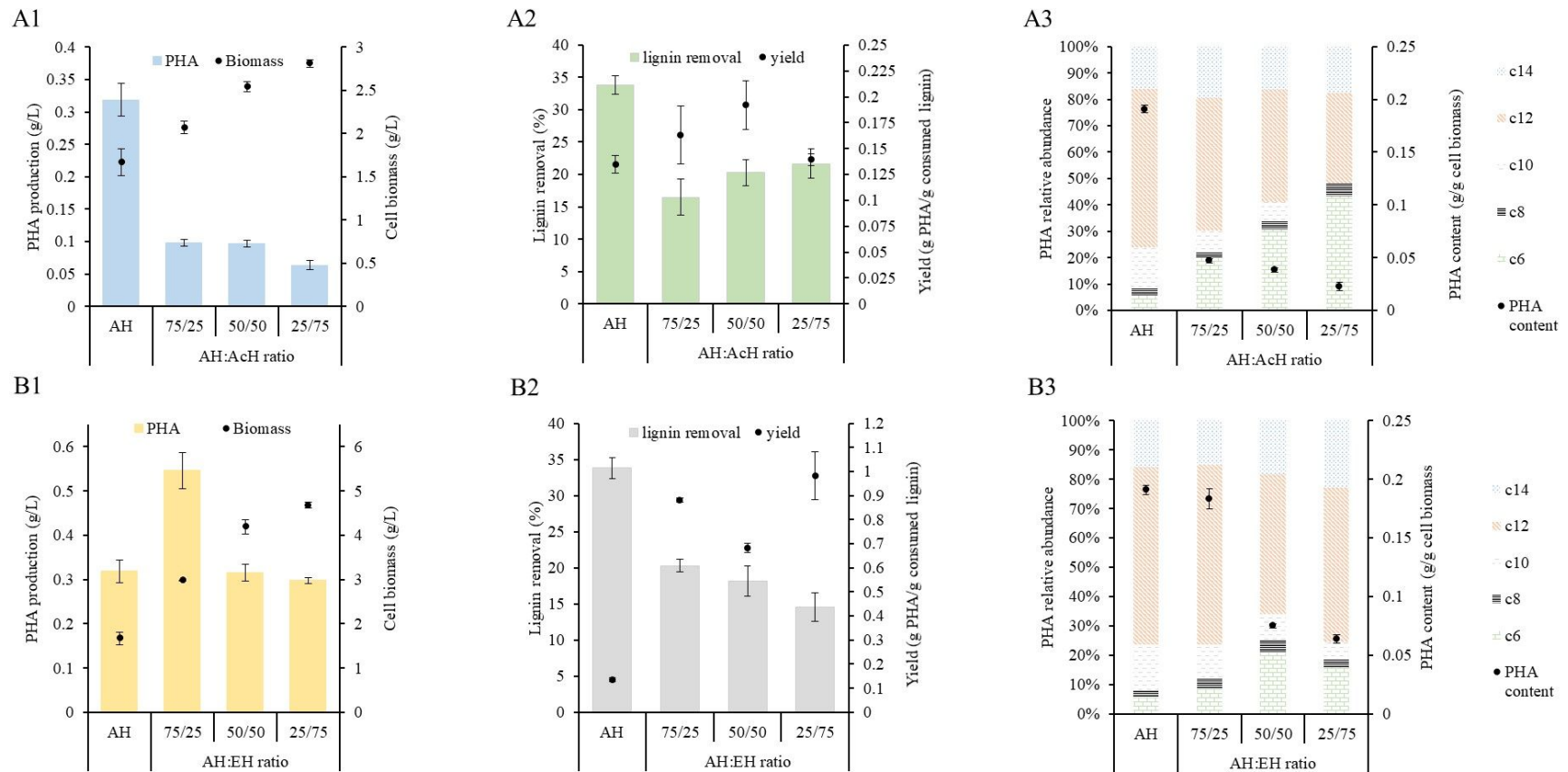


Fig. 4. Effect of A) acid (AcH) and B) enzymatic (EH) hydrolysates as co-substrates during the conversion of lignin (AH) to mcl-PHA in C1J4. Experiments were performed at 20 g/L SSC, pH 7 and initial $OD_{600}=0.3$; ratios are expressed in terms of SSC. A1 and B1) PHA and Cell biomass production; A2 and B2) lignin removal and PHA yield; A3 and B3) PHA relative abundance and PHA content.

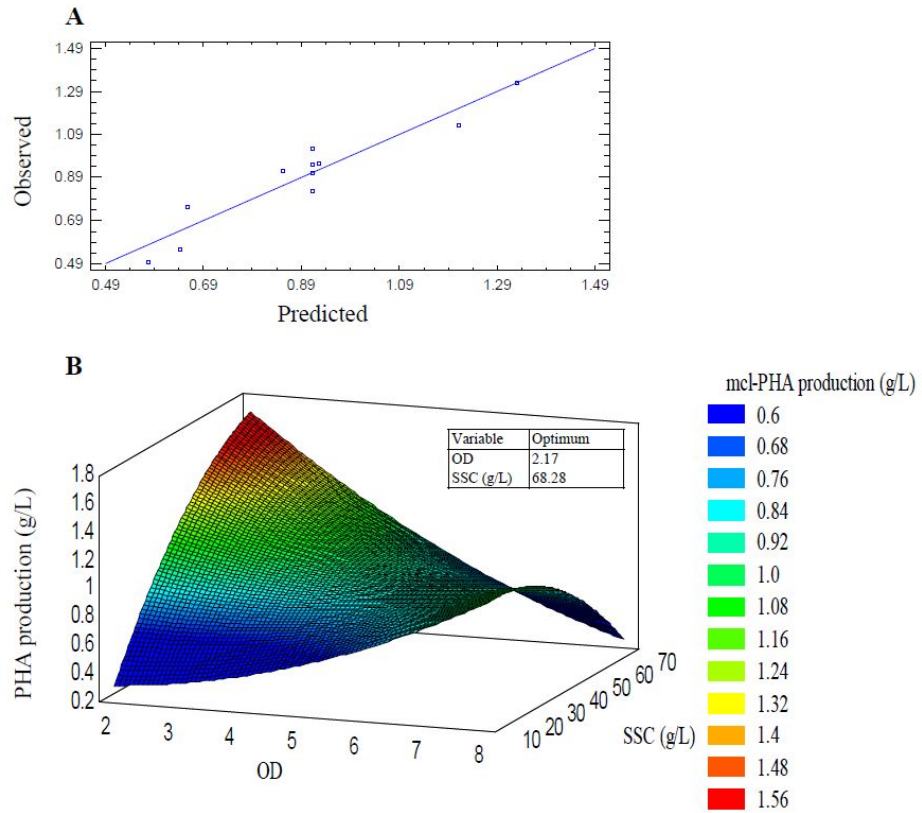


Fig. 5. A) Fitting of the quadratic model (Eqn. 2) to experimental data during the central composite design, and B) response surface obtained from the quadratic model (Eqn. 2) with optimal conditions displayed.

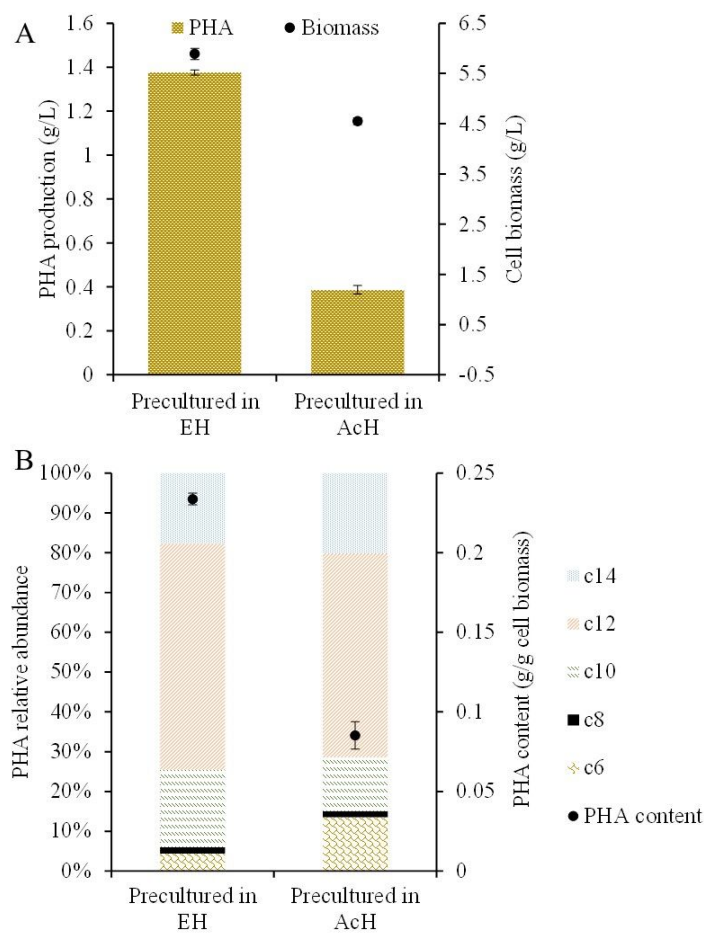


Fig. 6. Experimental evaluation of optimal conditions predicted by the quadratic model (Eqn. 2) by using acid (AcH) and enzymatic (EH) hydrolysates to pre-culture C1J4 strain. A) PHA and Cell biomass production; B) PHA relative abundance and PHA content.

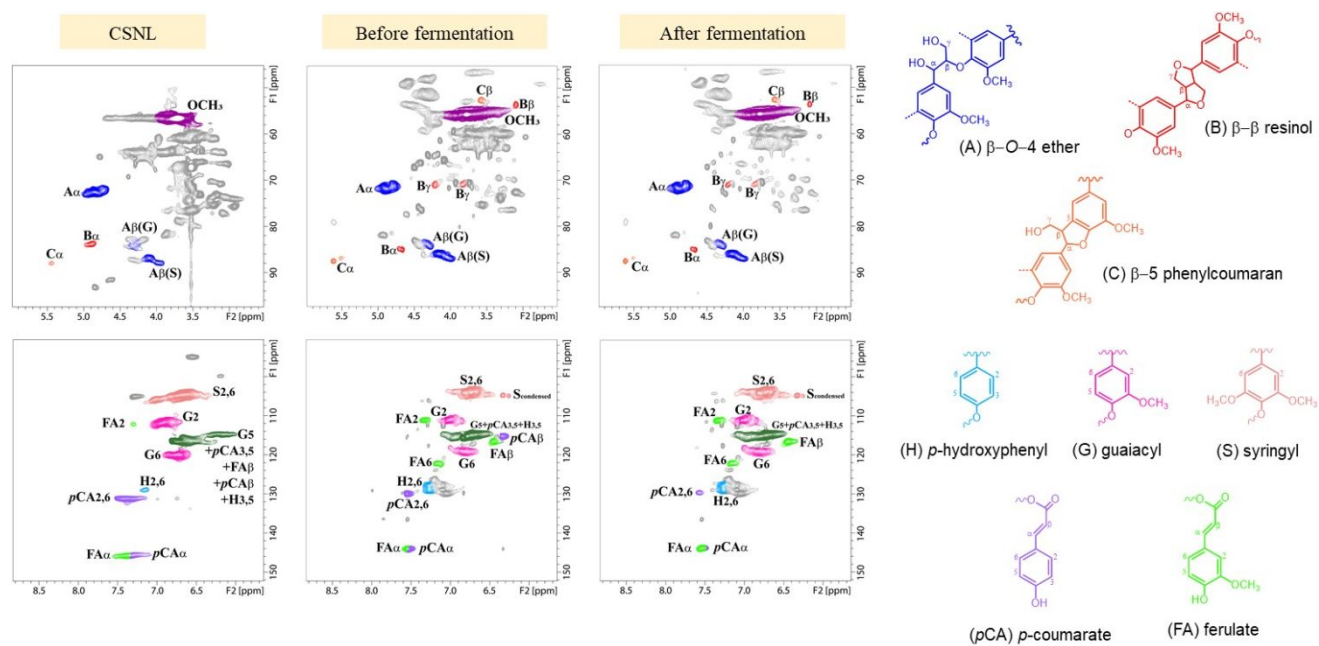


Fig. 7. The 2D HSQC NMR spectra of CSNL, and AH before and after fermentation.

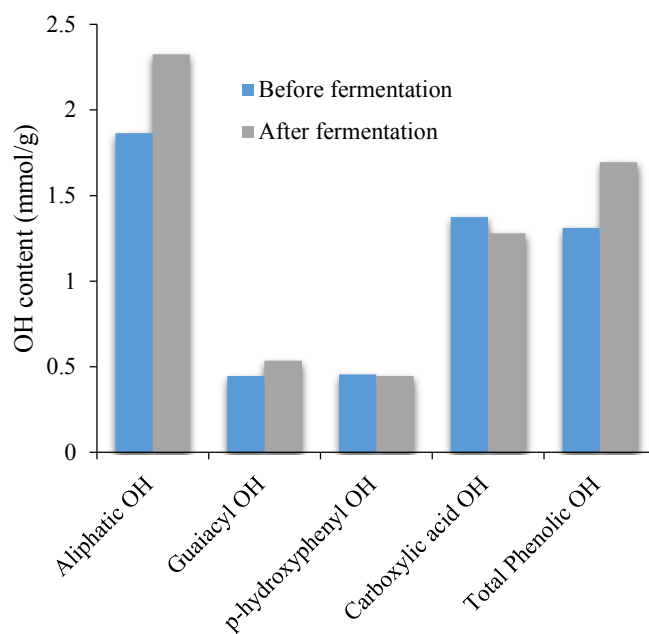


Fig. 8. Quantification of different hydroxyl group contents (mmol/g) in lignin samples before and after fermentation under optimal conditions determined by ^{31}P NMR spectra.